Spacecraft Doppler tracking as a narrow-band detector of gravitational radiation

Massimo Tinto* and J. W. Armstrong†
Jet Propulsion Laboratory, California Institute of Technology, Pasadena, California 91109
(Received 31 March 1998; published 27 July 1998)

We discuss a filtering technique for reducing the frequency fluctuations due to the troposphere, ionosphere, and mechanical vibrations of the ground antenna in spacecraft Doppler tracking searches for gravitational radiation. This method takes advantage of the sinusoidal behavior of the transfer function to the Doppler observable of these noise sources, which displays sharp nulls at selected Fourier components. The non-zero gravitational wave signal remaining at these frequencies makes this Doppler tracking technique the equivalent of a series of narrow-band detectors of gravitational radiation distributed across the low-frequency band. Estimates for the sensitivities achievable with the future Cassini Doppler tracking experiments are presented in the context of gravitational wave bursts, monochromatic signals, and a stochastic background of gravitational radiation. [S0556-2821(98)08116-8]

PACS number(s): 04.80.Nn, 07.60.Ly, 95.55.Ym

I. INTRODUCTION

Successful detection of gravitational waves (GWs) has important implications both for astronomy (where new information about astrophysical sources will be obtained) and for fundamental physics (where aspects of relativistic theories of gravity can be tested) [1]. Current experimental efforts involve three types of detector: resonant bars (narrow band devices sensitive at about one kilohertz center frequency), ground-based laser interferometers (broadband devices sensitive between 10s of Hz to ~few kilohertz), and Doppler tracking of distant spacecraft (sensitive at much lower frequencies, $\approx 10^{-5}$ to 10^{-1} Hz). For at least the next decade, until laser interferometers with very long arm lengths can be flown in space [2], the only experimental access to the low-frequency band will be by using Doppler tracking of spacecraft.

In the Doppler tracking technique, the Earth and an interplanetary spacecraft act as free test masses. The Doppler tracking system continuously measures their relative dimensionless velocity, $\Delta v/c = \Delta\nu/\nu_0$ (here Δv is the relative velocity, $\Delta\nu$ is the Doppler frequency fluctuation, and ν_0 is the nominal frequency of the microwave link). A gravitational wave of strain amplitude $h(t)$ propagating through the radio link causes small perturbations in the Doppler time series of $\Delta\nu(t)/\nu_0$. These perturbations are of order h and are replicated three times in the tracking record with a characteristic pattern that depends on the source-Earth-spacecraft angle [3]. These three events in the time series can be thought of as due to the GW buffeting the Earth, the GW buffeting the spacecraft, and the original Earth buffeting event transponded back to the Earth at a time $2L/c$ later, where L is the distance between the Earth and the spacecraft, and c is the speed of light. The sum of these three Doppler perturbations is zero. This overlap of the three events, and partial cancellation, occurs for GW pulses having widths larger than about L. This sets the lower band edge, for which one has full sensitivity, to be $\approx c/L$. Frequency stability of the master oscillator driving the Doppler system and finite signal-to-noise ratio on the radio links set the high frequency band limit to be ≈ 0.1 Hz.

Detection of GW signals in this millihertz band is complicated by various noises. The principal noise sources are [4–9]: ground electronics noise (including frequency standard and frequency distribution noise), antenna mechanical noise (unmodeled motion of the antenna), thermal noise (finite signal-to-noise ratio on the radio links), spacecraft noise (electronics and unmodeled motion of the spacecraft), and propagation noise (phase scintillation as the radio beams pass through irregularities in the troposphere, ionosphere, and the solar wind). Electronic and thermal noises can be made very small, and propagation noises can be mitigated through use of higher or multiple radio frequencies to suppress or remove entirely charged particle scintillation, and by employing water vapor radiometers to measure (and calibrate) tropospheric scintillation. Residual uncalibrated troposphere and antenna mechanical noise are expected to be leading noise sources in the future gravitational wave experiments performed with the Cassini project [9], a scientific mission to Saturn sponsored by the National Aeronautics and Space Administration (NASA), the European Space Agency (ESA), and the Italian Space Agency (ASI).

In this paper we show that, when the limiting noise sources in Doppler tracking data are the troposphere, ionosphere, and the mechanical vibrations of the ground antenna, one can take advantage of the sinusoidal behavior of their transfer functions to the Doppler observable to achieve lower noise levels. These transfer functions are all equal, but different from the ''3-pulse'' transfer function connecting the GW excitation to the Doppler response. The noise transfer function has sharp nulls at specific frequencies in the power spectrum. We show how this modulation of the noise spectrum can be exploited in a very robust way to improve the sensitivity of a Doppler GW search for bursts, sinusoids, and stochastic background waveforms.

In Sec. II we derive the transfer functions of the various noise sources affecting the Doppler response. After pointing out that the Cassini gravitational wave experiments will be

*Electronic address: mtinto@pop.jpl.nasa.gov
†Electronic address: John.W.Armstrong@jpl.nasa.gov

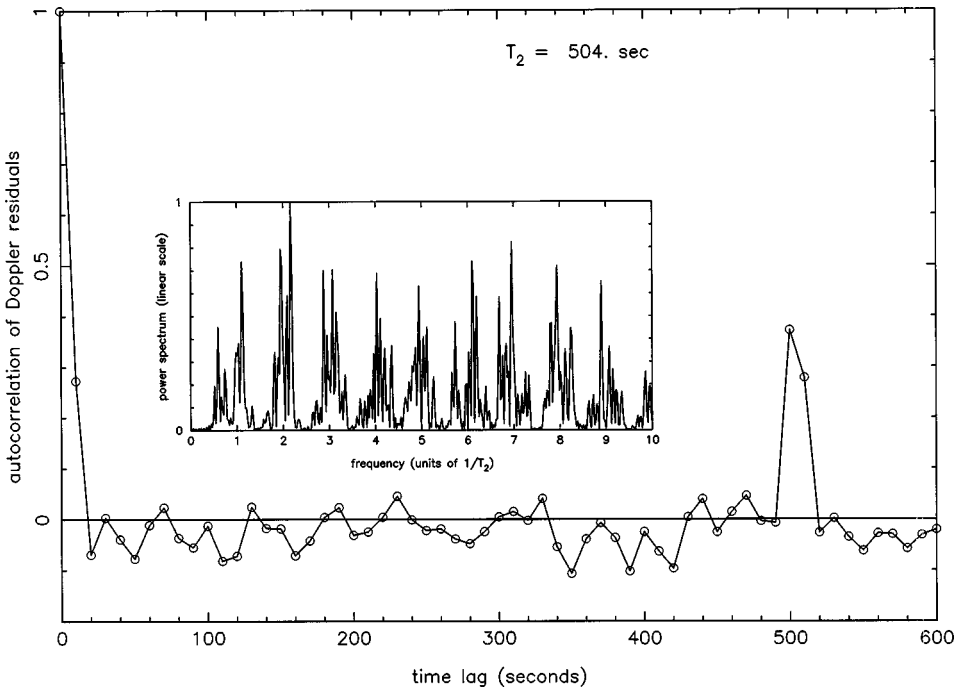

FIG. 1. The temporal autocorrelation function of 10-second time resolution Mars Global Surveyor Doppler data taken on April 17, 1997, when the two-way light time, $T_2=2L/c$, was equal to 504 seconds. The inset plot shows the power spectrum, with the frequency scale marked in units of $1/T_2$.

limited by the residual frequency fluctuations introduced by the troposphere, and the noise due to the mechanical vibrations of the ground antenna, we show how to effectively take advantage of the sinusoidal behavior of the transfer function of these noises in the Doppler observable in order to significantly reduce their magnitude at selected Fourier frequencies. In Sec. III we estimate the one-sided power spectral density of the noise for the Cassini gravitational wave experiments. Since Cassini will take advantage of a multilink radio system for removing the frequency fluctuations introduced by the interplanetary plasma in the Doppler data, we find a root-mean-squared noise (r.m.s.) sensitivity level to sinusoids of about 5.0×10^{-17} in the lower part of the band. In Sec. IV we present our comments and conclusions.

II. NOISES AND DOPPLER TRANSFER FUNCTIONS

The main noises affecting precision Doppler tracking observations map into the Doppler observable through characteristic transfer functions [6,10,11]. In a spacecraft Doppler tracking experiment, an interplanetary spacecraft coherently transponds back the signal it receives from the ground. That is, the spacecraft coherently generates the phase of the signal it transmits back to the Earth from the signal it receives from the ground. The contribution to the two-way Doppler tracking time series due to plasma fluctuations can be made small via high radio frequencies or multifrequency links [4,12,13]; the transfer function to the observable is given in [3,14]. The noise introduced by the frequency reference clock has instead the following transfer function [6,10,11]

$$\delta(t-2L/c)-\delta(t), \tag{2.1}$$

and produces an anticorrelation at time lag of $2L/c$. Tropospheric scintillation and antenna mechanical noises, which are non-dispersive and expected to be the leading noise sources in the Cassini Doppler data [9], each have the same transfer function to the Doppler observable

$$\delta(t-2L/c)+\delta(t). \tag{2.2}$$

For current generation precision Doppler experiments, utilizing approximately 8 GHz radio links, observations in the antisolar hemisphere have significant contributions from tropospheric and extended solar wind scintillation, while ionospheric, frequency standard, and antenna mechanical noise are secondary disturbances in the Doppler link [14]. As an example, in Fig. 1 we show the temporal autocorrelation function of 10-second time resolution Mars Global Surveyor (MGS) data taken on April 17, 1997, when the two-way light time $2L/c$ was equal to 504 sec. The clear positive correlation at time lag of 504 sec indicates that tropospheric scintillation and possibly fluctuations induced by mechanical vibrations of the ground antenna dominate the noise on this data set.

A consequence of the $\delta(t)+\delta(t-2L/c)$ transfer function is that the power spectrum, the Fourier transform of the autocorrelation function, will be modulated by $\cos^2(\pi f T_2)$, where $T_2=2L/c$ is the two-way light time. The inset plot in Fig. 1 shows the power spectrum of the MGS data, with frequency scale marked in units of $1/T_2$. No smoothing of the spectrum has been done and much of its spikiness is due to estimation error [15]. The cosine-squared modulation is however evident, showing that there are nulls at odd multiples of $1/(2T_2)$. At these frequencies, fluctuations from

other noise sources will dominate the power spectrum. If the spectral level of these secondary noises is low, there is a potentially large improvement in SNR for gravitational wave signals having Fourier power at the nulls of the troposphere-antenna mechanical transfer function. In its simplest form, filtering the data to pass a comb of narrow bands centered on the nulls of the cosine-squared transfer function blocks the troposphere-antenna mechanical noise while passing the power of gravitational wave signals at these frequencies. This is robust, in that nothing needs to be known about the signal except that it (by hypothesis) has power at odd multiples of $1/(2T_2)$. In this paper we estimate the SNR achievable with some waveforms, while practical effects such as the change in T_2 over an observing interval, are presented in the next section.

III. APPLICABILITY AND PERFORMANCE

From the considerations made in the previous section about the transfer functions of the various noise sources affecting Doppler tracking, we can write the Doppler response $y(t)$ to a gravitational wave in the following form [6,11]:

$$\begin{aligned} y(t) &\equiv \frac{\Delta\nu(t)}{\nu_0} \\ &= -\frac{(1-\mu)}{2}h(t) - \mu h(t-(1+\mu)L) \\ &\quad + \frac{(1+\mu)}{2}h(t-2L) + C(t-2L) - C(t) + 2B(t-L) \\ &\quad + T(t-2L) + T(t) + A_E(t-2L) + A_{sc}(t-L) \\ &\quad + TR(t-L) + EL(t) + P(t), \end{aligned} \tag{3.1}$$

where $h(t)$ is equal to

$$h(t) = h_+(t)\cos(2\phi) + h_\times(t)\sin(2\phi). \tag{3.2}$$

Here $h_+(t)$, $h_\times(t)$ are the wave's two amplitudes defined with respect to two axis, (X,Y), chosen in the plane of the wave, (θ,ϕ) are the polar angles describing the location of the spacecraft with respect to the right-handed triad (X,Y,Z) (with Z orthogonal to the $X-Y$ plane), μ is equal to $\cos\theta$, and the speed of light c has been chosen to be equal to 1.

We have denoted with $C(t)$ the random process associated with the frequency fluctuations of the clock, $B(t)$ the joint effect of the noise from buffeting of the probe by non-gravitational forces and from the antenna of the spacecraft, $T(t)$ the joint frequency fluctuations due to the troposphere, ionosphere and ground antenna, $A_E(t)$ the noise of the radio transmitter on the ground, $A_{sc}(t)$ the noise of the radio transmitter on board, $TR(t)$ the noise due to the spacecraft transponder, $EL(t)$ the noise from the electronics on the ground, and $P(t)$ the fluctuations due to the interplanetary plasma.

Since the frequency fluctuations induced by the plasma are inversely proportional to the square of the radio frequency, by using high frequency radio signals or by monitoring two different radio frequencies transmitted to the spacecraft and coherently transmitted back to Earth, this noise source can be suppressed to very low levels or entirely removed from the data respectively [12]. Searches for gravitational radiation with Doppler tracking utilizing only one radio frequency are usually performed around solar opposition in order to minimize the frequency fluctuations induced by the plasma [16]. If the frequency of the radio signal is Ka-Band (32 GHz) (as it will be the case with the Cassini gravitational wave experiments), and the tracking is performed at solar opposition, at 1000 seconds integration time the plasma noise is equal to about 7.0×10^{-16} [8]. If dual frequencies are used instead, such as X ($\approx$8 GHz) and Ka bands for instance, by linearly combining the Doppler data at these two radio frequencies we can entirely remove the first order frequency fluctuations due to the plasma. The magnitude of the first higher order term is equal to about 7.0×10^{-30} [12], making it totally negligible with respect to other non-dispersive noise sources [8].

If we denote with $\tilde{y}(f)$ the Fourier transform of the Doppler response $y(t)$ calculated over the time of observation 2τ, this is defined as follows:

$$\tilde{y}(f) = \int_{-\tau}^{\tau} y(t)e^{2\pi i f t}dt, \tag{3.3}$$

and at the Fourier frequencies

$$f_k = \frac{(2k-1)}{2T_2}; \quad k = 1,2,3,\ldots. \tag{3.4}$$

Equation (3.1) can be rewritten in the following approximate form [11]:

$$\begin{aligned} \tilde{y}(f_k) \approx & [-1 + i(-1)^k \mu e^{\pi/2\, i(2k-1)\mu}]\tilde{h}(f_k) \\ & - 2\tilde{C}(f_k) + \tilde{T}(f_k)\left(\frac{\pi i L}{2\tau}\right) \\ & + i(-1)^{k+1}[2\tilde{B}(f_k) + \widetilde{TR}(f_k) + \widetilde{A_{sc}}(f_k)] \\ & - \widetilde{A_E}(f_k) + \widetilde{EL}(f_k) + \tilde{P}(f_k). \end{aligned} \tag{3.5}$$

In Eq. (3.5) we have assumed that the time dependence of the two-way light time is such that during the time scale 2τ over which the Fourier transform is performed the frequencies f_k change by an amount smaller than the frequency resolution $\Delta f = 1/2\tau$. In practical experiments this is not true. In the case of MGS, for example, the time variation of T_2 causes the position of the xylophone nulls to move by more than the Fourier resolution bin in coherent integrations that are longer than about 8 hours. More relevant, however, is the magnitude of the T_2-correlated noise with respect to that of the other noise sources. The variation of T_2 smears the spectrum of the T_2-correlated noise, reducing the depth-of-null at the xylophone frequencies. The T_2-correlated noise level, however, is still reduced to that of the remaining noise sources in the neighborhood of the xylophone frequencies. This will be the case for the Cassini experiments.

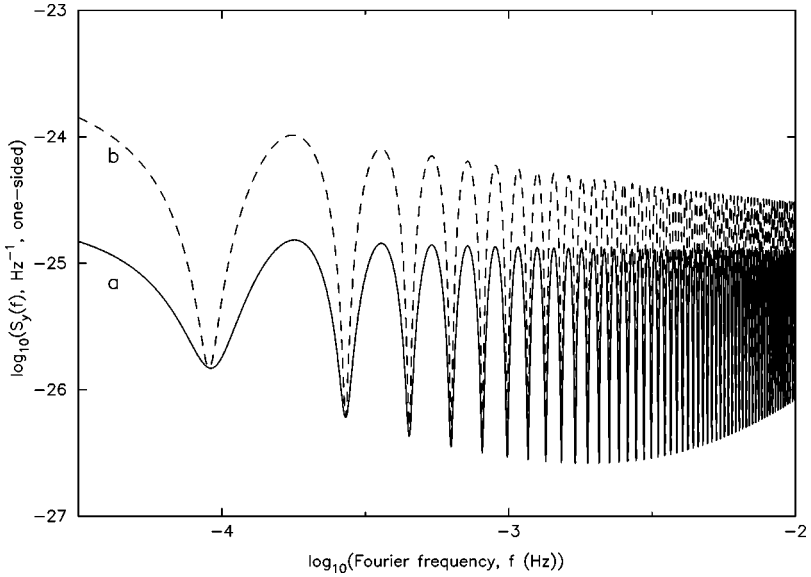

FIG. 2. The estimated one-sided power spectral density of the noise that will affect the Cassini Doppler data. Curve ''a'' represents the configuration in which 80 percent of the noise due to the troposphere has been calibrated and removed by means of water vapor radiometry; curve ''b'' corresponds to the configuration without calibration of the troposphere.

We note from Eq. (3.5) that the Fourier components of the random process T at the frequencies f_k are reduced in magnitude by the factor $(\pi L)/(2c\tau)$. With a two-way light time of about five hundred seconds, and an observation time of eight hours, the reduction factor for the frequency fluctuations due to the troposphere, ionosphere, and the mechanical fluctuations of the ground antenna, is equal to 2.7×10^{-2} for the MGS data. In the case of Cassini instead this factor could be as small as 2.5×10^{-3} for the first opposition (40 days integration, distance to the spacecraft 5.5 a.u.).

In Eq. (3.5) we provide also the antenna pattern of the remaining signal at the frequencies f_k. As expected it is equal to zero when $\mu=\pm1$, and has a maximum value of 1 at $\mu=0$. For sources randomly distributed over the sky, like in the case of a stochastic background of gravitational waves, we can assume the angles (θ,ϕ) to be random variables uniformly distributed over the sphere and over the interval $[0,2\pi]$ respectively. The average over (θ,ϕ) of the antenna pattern given in Eq. (3.5) is equal to zero, while its variance, which we will denote with $\Sigma_h^2(k)$, is equal to the following monotonically increasing function of the integer k

$$\Sigma_h^2(k)=\frac{4}{3}-\frac{8}{\pi^2(2k-1)^2},\quad k=1,2,3,\ldots. \tag{3.6}$$

From Eq. (3.5) we can derive the expression for the expected one-sided power spectral density $S_y(f_k)$ of the noise in the Doppler response $y(t)$ at the frequencies f_k. Under the assumption that the random processes representing each noise source are uncorrelated with each other, and their one-sided power spectral densities are as given in [8,9], we can plot $S_y(f_k)$ for different radio tracking configurations. Since Cassini will be simultaneously tracked at X and Ka bands only at one of the three complexes of the Deep Space Network (DSN), and tracking at the remaining two DSN facilities will be performed at X-Band, we conclude that for one third of the duration of these gravitational wave experiments the effects of the interplanetary plasma can be entirely removed from the Doppler data, while for two thirds of the observing time the plasma noise will be one of the leading noise sources in the Doppler data. In Fig. 2 we plot the one-sided spectral density of the noise in the Cassini Doppler residual, from which the interplanetary plasma scintillations have been removed. The continuous-line curve corresponds to the configuration in which eighty percent of noise due to the troposphere has been calibrated out with water vapor radiometry, while the dotted-line assumes no calibration of the troposphere. Since the power of the frequency fluctuations due to the troposphere are reduced, at the frequencies f_k, to a level smaller than the remaining noise sources, we see why the two curves plotted in Fig. 2 coincide at the frequencies f_k.

Figure 2 also allows us to estimate the signal-to-noise ratios for various waveforms. Gravitational waves can be classified into three categories, depending on their temporal behavior and their time duration relative to the time of observation. A complete review of gravitational wave sources, and estimates of the corresponding strengths of interest in the millihertz frequency band, are given in Ref. [1]. Here we will briefly summarize some of the anticipated sources of gravitational waves and compare the amplitude of the waves they are expected to radiate to the noise spectral levels presented in Fig. 2 for the Cassini experiments.

Gravitational wave bursts in the millihertz frequency band could be emitted during different astrophysical scenarios. A collapse of a star cluster to form a supermassive black hole, for instance, might generate a waveform whose dominant spectral components coincide with the frequencies at which the effects of the troposphere and mechanical vibrations of the ground antenna are suppressed.

Another astrophysical scenario implying the emission of a gravitational wave burst is the fall of small black holes into a super massive black hole, as it might happen at the end of the merger of two galaxies hosting at their centers a black hole. Although the temporal dependence of the gravitational wave burst radiated during the merger is unknown, the radiation emitted by the newly formed hole during the settling process can be described mathematically quite well [17,18]. The radiation in this case is strongly dominated by the black-hole quasinormal modes, whose frequencies and damping times depend on the mass of the hole and its angular momentum. The strongest and most slowly damped of these modes is expected to be the fundamental, whose gravitational wave tensor can be written as follows [17]

$$h_{ij}(t)=\begin{cases} e_{ij}h_0 e^{-(t-t_s)/\tau_0}\sin[2\pi f_s(t-t_s)], & \text{for } t\geqslant t_s \\ 0 & \text{for } t<t_s \end{cases}, \tag{3.7}$$

where e_{ij} is the polarization tensor, h_0 is the wave's amplitude at its time of arrival t_s, and f_s and τ_0 are the quasinormal mode's frequency and damping time respectively. The analytic expressions for the amplitude h_0, the frequency f_s of the damped mode, and the damping time τ_0 are as follows [17,18]

$$h_0=\frac{1}{r}\left(\frac{G}{\pi^2 c^3}\frac{\Delta E}{f_s}\right)^{1/2} \tag{3.8}$$

$$f_s=\frac{c^3}{2\pi MG}[1-0.63(1-a)^{0.3}] \tag{3.9}$$

$$\pi f_s\tau_0=2(1-a)^{-0.45}\geqslant 2. \tag{3.10}$$

Here r is the physical distance to the black-hole, ΔE is the energy radiated in the form of gravitational waves over the time scale $1/f_s$, a is the dimensionless rotation parameter, and M is the mass of the black-hole. When a approaches 1 we have a relativistically rotating black-hole, while $a=0$ corresponds to the radiation from a perturbed Schwarzschild hole [17]. Note that, in order for the signal to perform one oscillation before getting damped, the black-hole must rotate with an angular momentum a as large as 0.633 [the right-hand-side of Eq. (3.10) must be equal to π in order to have $\tau_0=1/f_s$].

It is well known that the largest signal-to-noise ratio is achieved by applying matched filtering to the data [19]. We have calculated the signal-to-noise ratio achievable with matched filtering for the quasi-normal mode waveform given by Eqs. (3.7)–(3.10) in the presence of noise having spectrum as in Fig. 2. Under the assumption that the propagation direction of the signal is orthogonal to the radio beam, the signal-to-noise ratio $[\mathrm{SNR}(f_s,a)]$ given by matched filtering is [18]

$$\mathrm{SNR}(f_s,a)=\frac{h_0^2 f_s^2}{2\pi^2}\int_{-\infty}^{+\infty}\times\frac{\sin^2\left(\frac{\pi f}{2f_s}\right)}{S_y(f)[f^4-Af^2+B]}df, \tag{3.11}$$

where we have denoted with A and B the following functions:

$$A=2\left[1-\frac{(1-a)^{9/10}}{16}\right]f_s^2 \tag{3.12}$$

$$B=\left[1+\frac{(1-a)^{9/10}}{16}\right]^2 f_s^4. \tag{3.13}$$

If we assume the energy ΔE emitted in the form of gravitational radiation to be proportional to the rest energy of the black-hole ($\Delta E=\epsilon Mc^2$), by substituting Eq. (3.9) into Eq. (3.8) it is easy to derive the following expression for the wave's amplitude h_0:

$$h_0=\frac{c}{\pi r f_s}\left\{\frac{[1-0.63(1-a)^{0.3}]\epsilon}{2\pi}\right\}^{1/2}. \tag{3.14}$$

Note from Eq. (3.14) that, for a fixed angular momentum a, fractional radiated energy ϵ, and source distance r, the amplitude of the wave increases inversely with the center frequency, f_s. This is because the mass of the system is inversely proportional to f_s [Eq. (3.9)]. For example, for a frequency $f_s=10^{-4}$, the corresponding mass of the Schwarzschild black hole is about $10^8\ M_\odot$.

Owing to the spectral modulation, the signal-to-noise ratio of the filter matched to a quasi-normal mode waveform will vary with center frequency, f_s. In Figs. 3(a,b) we plot this signal-to-noise ratio versus f_s for non-rotating ($a=0$) and highly-rotating ($a=0.99$) waveforms for the two noise spectra given in Fig. 2. Note that the signal-to-noise ratios have been plotted for $\epsilon=10^{-4}$ and $r=1$ Mpc; the explicit dependence of the SNR on these two parameters is proportional to $\epsilon^1 r^{-2}$.

As an example application of Fig. 3, consider gravitational radiation from quasinormal mode perturbations of a black hole in the Andromeda galaxy. There is evidence that Andromeda ($r=770$ kpc) has a $(1-5)\times 10^7\ M_\odot$ black hole [20]. For a rapidly-rotating $5\times 10^7\ M_\odot$ black hole, $f_s=0.00054$ Hz. The Cassini first opposition has $\theta\approx 117°$ with respect to Andromeda, giving good angular response. To achieve a matched filter SNR of 10, the quasinormal mode vibrations of the black hole in Andromeda requires an efficiency $\epsilon\approx 3\times 10^{-5}$. For more massive holes (up to $\approx 10^9\ M_\odot$) in the Virgo cluster or a less massive hole ($\approx 10^6\ M_\odot$) at the Galactic center, the quasinormal mode radiation efficiency would need to be comparable, $\epsilon\approx 10^{-4}$, to achieve SNR=10 with Cassini.

Let us now turn to the two remaining classes of gravitational waveforms, namely sinusoids and stochastic backgrounds of gravitational radiation. In the case of the stochas-

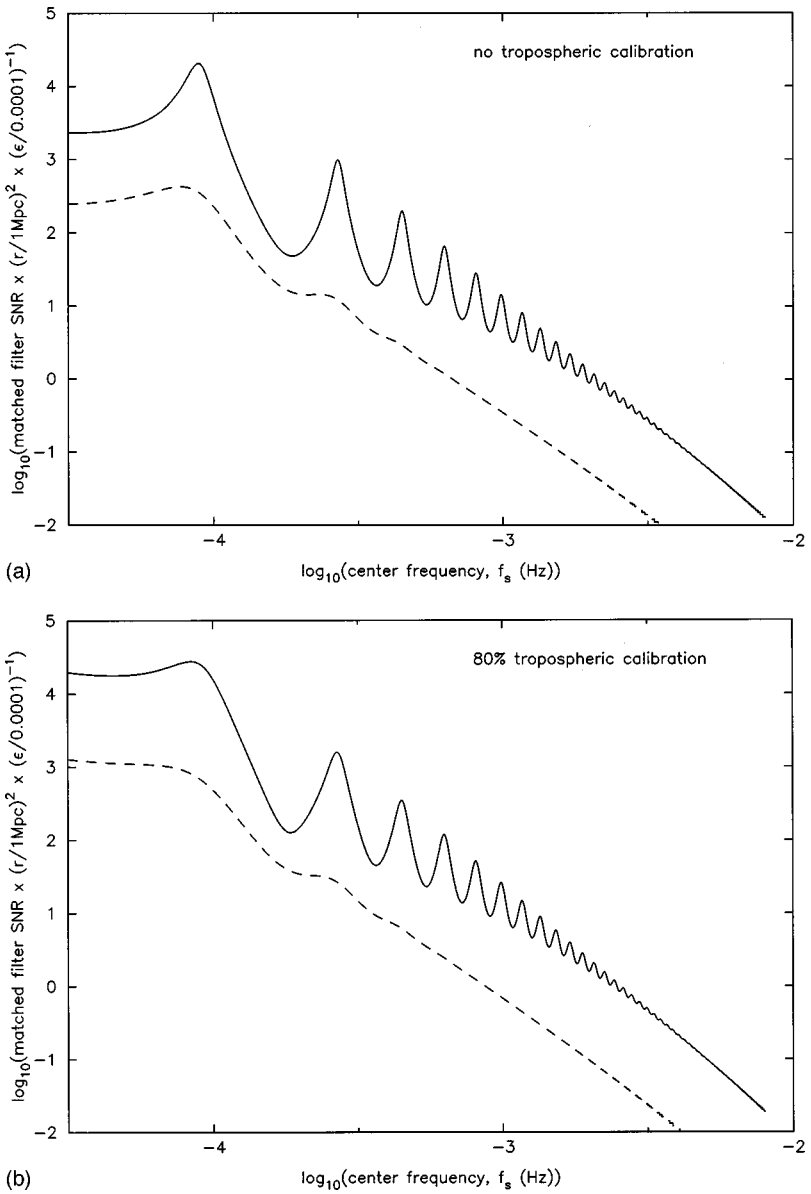

FIG. 3. Signal-to-noise ratio (SNR) for matched filtering to quasinormal mode gravitational waves incident at right angles to the earth-spacecraft line, as a function of the normal mode frequency f_s and two values of the angular momentum parameter, $a=0$ (dashed) and $a=0.99$ (solid). (a) SNR for no tropospheric corrections. (b) SNR for 80 percent of the tropospheric noise removed.

tic background with bandwidth equal to center frequency, the sensitivity of the Doppler data at the frequencies f_k is given by the expected root-mean-squared (r.m.s.) noise level $\sigma(f_k)$ of the frequency fluctuations in the bins of width f_k. This is given by the following expression:

$$\sigma(f_k)=[S_y(f_k)f_k]^{1/2},\quad k=1,2,3,\ldots, \tag{3.15}$$

where $S_y(f_k)$ is the one-sided power spectral density of the noise sources in the Doppler response $y(t)$ at the frequency f_k, as given in Fig. 2.

When searching for a stochastic background of gravitational radiation, best sensitivity is achieved at the lowest xylophone frequency. For the first Cassini opposition, $f_1=9\times10^{-5}$ Hz. We get an energy density per unit logarithmic frequency and per unit critical energy density Ω [1] equal to $\approx10^{-2}$, after taking into account the effect of the r.m.s. antenna pattern $(\Sigma_h^2)^{1/2}(k=1)$ given in Eq. (3.6). Subsequent Cassini oppositions have lower first xylophone frequencies, giving $\Omega\approx4\times10^{-3}$. Cassini will give the best observational upper limit on a gravitational wave background in the millihertz band.

Sources of sinusoidal gravitational waves in the millihertz frequency band are expected to be spiraling binary systems containing black holes [21]. As such a system evolves, the frequency of the emitted radiation slowly increases due to gravitational radiation reaction. If the source radiates near one of the frequencies f_k and is sufficiently far from coalescence then it will radiate predominantly as a sinusoid. In the millihertz band we can describe mathematically the radiation they emit quite accurately in the Newtonian approximation. In this framework the maximum amplitude radiated by the

system, and the time it spends around a specified frequency f are given by the following expressions:

$$h(t)=\frac{4G^{5/3}}{c^4}\frac{\mu}{r}[\pi f(t)M]^{2/3} \tag{3.16}$$

$$\frac{f(t)}{\dot{f}(t)}\equiv\eta(t)=\frac{5c^5}{96G}\frac{[\pi f(t)]^{-8/3}}{\mu(GM)^{2/3}}, \tag{3.17}$$

where r is the physical distance to the binary system, G is the gravitational constant, c is the speed of light, η is the characteristic time spent by the system around the frequency $f(t)$, and μ and M are the reduced and total mass of the system respectively. Since the maximum signal-to-noise ratio at the frequencies f_k will be achieved when the signal's frequency does not change more than the frequency resolution Δf of the Fourier transform, the following condition must be satisfied:

$$\dot{f}2\tau<\frac{1}{2\tau}. \tag{3.18}$$

If we divide both sides of Eq. (3.18) by one of the frequencies f_k, we obtain the following inequality relating the time spent by the signal's frequency around the frequency f_k, η_k, to the integration time 2τ:

$$\eta_k>f_k(2\tau)^2. \tag{3.19}$$

Note that, the smaller the frequency at which we will perform our observation the easier will be to have binary systems radiating sinusoidally over the period of observation. At 9.0×10^{-5} Hz, and with an observation time of 40 days, we will be able to integrate coherently for signals that spend about 4.0×10^8 seconds around such a frequency. If we now multiply Eqs. (3.16), (3.17), we note that the product $h\eta$ does not depend on the mass of the system, and is a function only of the frequency f and the physical distance r [22]:

$$h\times\eta=\frac{5c}{24r(\pi f)^2} \tag{3.20}$$

By assuming equal mass objects, and the smallest η consistent with Eq. (3.19) (4.0×10^8 seconds), the implied mass for a 9.0×10^{-5} Hz radiation frequency is $\approx10^5\ M_\odot$. For this value of η, and an equivalent sinusoidal sensitivity of $\approx10^{-16}$ at f_1, we find that such a system could be observed with SNR$>$10 to a distance $\approx$100 kpc, which includes many members of the Local Group.

IV. CONCLUSIONS

The main result of our analysis is that, during searches for gravitational radiation, it is possible to reduce the noise of the troposphere, ionosphere, and mechanical vibrations of the ground antenna at selected Fourier components of the power spectrum of two-way Doppler tracking data. An equivalent sinusoidal signal sensitivity of $\approx5.0\times10^{-17}$ at a frequency of 2.0×10^{-3} has been estimated for the future Cassini gravitational wave experiments, which will be performed starting in November 2001. For quasi-normal mode burst waves, we analyzed Cassini's sensitivity as a function of dominant wave frequency, radiation efficiency, angular momentum, and distance. We found that fractional radiated energy ϵ greater than about 3×10^{-5} is required for reliable detections of quasinormal mode radiation from known massive black hole candidates. For a stochastic background of gravitational radiation, at the xylophone frequency $f_1=9\times10^{-5}$ Hz we estimated an energy density per unit logarithmic frequency and per unit critical energy density Ω equal to $\approx10^{-2}$ with the expected Cassini noise spectrum.

The data analysis technique presented in this paper can be extended to a configuration with two spacecraft tracking each other through microwave or laser links in order to minimize the noise of the onboard frequency references. Future space-based laser interferometric detectors of gravitational waves [2], for instance, could implement this technique as a backup option, if failure of some of their components would make the normal interferometric operation impossible. In this case, the secondary noises are much smaller than the principal noise source, leading to very dramatic sensitivity improvements at the xylophone frequencies. We will explore in a forthcoming paper the strain sensitivities achievable with spacecraft to spacecraft Doppler tracking systems.

ACKNOWLEDGMENTS

This research was performed at the Jet Propulsion Laboratory, California Institute of Technology, under contract with the National Aeronautics and Space Administration. It is a pleasure to thank B. Bertotti, F. B. Estabrook, L. Iess, and H. D. Wahlquist for ongoing discussion of all aspects of the low-frequency gravity wave search problem.

[1] K. S. Thorne, in *Three Hundred Years of Gravitation*, edited by S. W. Hawking and W. Israel (Cambridge University Press, Cambridge, England, 1987).

[2] LISA: Laser Interferometer Space Antenna for the detection and observation of gravitational waves, Pre-Phase A Report. Max-Planck-Institute für Quantenoptic, Garching bei München, **MPQ 208** (1996).

[3] F. B. Estabrook and H. D. Wahlquist, Gen. Relativ. Gravit. **6**, 439 (1975).

[4] H. D. Wahlquist, Search for Low-Frequency Gravitational Waves using the Cassini Radio Science System Facility, Cassini Project, JPL (1990) (unpublished). See also H. D. Wahlquist, J. D. Anderson, F. B. Estabrook, and K. S. Thorne,

Atti. Accad. Naz. Lincei, Cl. Sci. Fis. Mat. Nat. Rend. **34**, 335 (1977).

[5] F. B. Estabrook, Proposal for Participation on Radio Science/ Celestial Mechanics Team for an Investigation of Gravitational Radiation, Galileo Project, JPL (1976) (unpublished). See also F. B. Estabrook, R. W. Hellings, H. D. Wahlquist, J. D. Anderson, and R. S. Wolff, in *Sources of Gravitational Radiation*, edited by L. Smarr (Cambridge University Press, Cambridge, England, 1979).

[6] J. W. Armstrong, in *Gravitational Wave Data Analysis*, edited by B. F. Schutz (Kluwer, Dordrecht, 1989).

[7] T. K. Peng, J. W. Armstrong, J. C. Breidenthal, F. F. Donivan, and N. C. Ham, Acta Astron. **17**, 321 (1988).

[8] A. L. Riley, D. Antsos, J. W. Armstrong, P. Kinman, H. D. Wahlquist, B. Bertotti, G. Comoretto, B. Pernice, G. Carnicella, and R. Giordani, Cassini Ka-Band Precision Doppler and Enhanced Telecommunications System Study, Pasadena, California, 1990 (unpublished).

[9] M. Gatti, M. Tinto, G. Morris, R. Perez, S. Petty, P. Cramer, P. Kuhnle, M. Gudim, D. Rogstad, L. Riley, and M. Marina, Cassini Radio Science Ground System Cost and Schedule Review, Pasadena, California, 1997 (unpublished).

[10] R. F. C. Vessot and M. W. Levine, Gen. Relativ. Gravit. **10**, 181 (1979).

[11] M. Tinto, Phys. Rev. D **53**, 5354 (1996).

[12] B. Bertotti, G. Comoretto, and L. Iess, Astron. Astrophys. **269**, 608 (1993).

[13] L. Iess, P. Bonifazi, B. Bertotti, and G. Comoretto, Nuovo Cimento C **10**, 235 (1987).

[14] J. W. Armstrong, Radio Science, 1998.

[15] G. M. Jenkins and D. G. Watts, *Spectral Analysis and Its Applications* (Holden-day, San Francisco, 1968).

[16] J. W. Armstrong, R. Woo, and F. B. Estabrook, Astrophys. J. **230**, 570 (1979).

[17] L. P. Grishchuk, Sov. Phys. Usp. **31**, 940 (1988).

[18] F. Echeverria, Phys. Rev. D **40**, 3194 (1989).

[19] C. W. Helstrom, *Statistical Theory of Signal Detection* (Pergamon, Oxford, 1968).

[20] T. R. Lauer *et al.*, Astron. J. **106**, 1436 (1993).

[21] H. D. Wahlquist, Gen. Relativ. Gravit. **19**, 1101 (1987).

[22] B. F. Schutz, Nature (London) **323**, 310 (1986).